Mon. Not. R. Astron. Soc. **000**, 1–13 (2006) Printed 5 February 2008 (MN LATEX style file v2.2)

Photometry of Magellanic Cloud clusters with the Advanced Camera for Surveys - II. The unique LMC cluster ESO 121-SC03

A. D. Mackey,[1⋆] M. J. Payne[1] and G. F. Gilmore[1]
[1] *Institute of Astronomy, University of Cambridge, Madingley Road, Cambridge CB3 0HA*

Accepted 2006 March 17. Received 2006 March 17; in original form 2006 March 03.

ABSTRACT

We present the results of photometric measurements from images of the LMC cluster ESO 121-SC03 taken with the Advanced Camera for Surveys on the *Hubble Space Telescope*. Our resulting colour-magnitude diagram (CMD) reaches 3 magnitudes below the main-sequence turn-off, and represents by far the deepest observation of this cluster to date. We also present similar photometry from ACS imaging of the accreted Sagittarius dSph cluster Palomar 12, used in this work as a comparison cluster. From analysis of its CMD, we obtain estimates for the metallicity and reddening of ESO 121-SC03: [Fe/H] $= -0.97 \pm 0.10$ and $E(V-I) = 0.04 \pm 0.02$, in excellent agreement with previous studies. The observed horizontal branch level in ESO 121-SC03 suggests this cluster may lie 20 per cent closer to us than does the centre of the LMC. ESO 121-SC03 also possesses a significant population of blue stragglers, which we briefly discuss. Our new photometry allows us to undertake a detailed study of the age of ESO 121-SC03 relative to Pal. 12 and the Galactic globular cluster 47 Tuc. We employ both vertical and horizontal differential indicators on the CMD, calibrated against isochrones from the Victoria-Regina stellar models. These models allow us to account for the different α-element abundances in Pal. 12 and 47 Tuc, as well as the unknown run of α-elements in ESO 121-SC03. Taking a straight error-weighted mean of our set of age measurements yields ESO 121-SC03 to be 73 ± 4 per cent the age of 47 Tuc, and 91 ± 5 per cent the age of Pal. 12. Pal. 12 is 79 ± 6 per cent as old as 47 Tuc, consistent with previous work. Our result corresponds to an absolute age for ESO 121-SC03 in the range $8.3 - 9.8$ Gyr, depending on the age assumed for 47 Tuc, therefore confirming ESO 121-SC03 as the only known cluster to lie squarely within the LMC age gap. We briefly discuss a suggestion from earlier work that ESO 121-SC03 may have been accreted into the LMC system.

Key words: galaxies: star clusters – globular clusters: individual: ESO 121-SC03, Palomar 12 – Magellanic Clouds

1 INTRODUCTION

The Large Magellanic Cloud (LMC) contains an extensive population of massive star clusters, with ages ranging from the very newly formed (e.g., R136 with age $\sim 3-4$ Myr) to those with ages comparable to the Galactic globular clusters (e.g., Hodge 11). These objects are extremely useful not only for studies of cluster development, but also for tracing the formation history of the LMC and its related kinematic, structural, and chemical evolution.

Of particular interest in this respect is the distribution of star cluster ages. A number of authors have explicitly demonstrated, using high quality colour-magnitude diagrams, that the oldest globular clusters in the LMC are coeval with the oldest Galactic globular clusters, to within ~ 1 Gyr (e.g., Johnson et al. 1999; Olsen et al. 1998; Mackey & Gilmore 2004). With the recent addition of NGC 1928 and 1939, the census of objects constituting this group of ancient clusters numbers 15 (Mackey & Gilmore 2004). There also exists a very substantial population of young and intermediate age clusters; however, examination of the age distribution reveals an almost complete dearth of clusters older than ~ 3 Gyr but younger than the ancient ensemble (e.g., Rich et al. 2001). This curious distribution constitutes the well known LMC cluster age-gap. Recent research aimed at explaining the existence of the age-gap has focused on the

⋆ E-mail: dmackey@ast.cam.ac.uk

impact of the periodic strong tidal interactions between the LMC and its companion the Small Magellanic Cloud (SMC) (Bekki et al. 2004).

Only one cluster is suspected to lie within the age gap. This is the remote northern LMC member ESO 121-SC03, which lies at a projected angular separation of $\sim 10^{\circ}$ from the LMC centre. ESO 121-SC03 was first studied in detail by Mateo et al. (1986), who used BV photometry to estimate an age in the range $8 - 10$ Gyr. Subsequent work has not altered this conclusion (e.g., Sarajedini et al. 1995; Geisler et al. 1997; Bica et al. 1998). Given its apparently unique age, and interesting spatial location, ESO 121-SC03 clearly constitutes an object worthy of detailed study. We were therefore surprised to discover that it apparently has not been the subject of deep high-resolution imaging: we could only locate two independent published CMDs in the literature – the BV photometry of Mateo et al. (1986), and the Washington photometry of Geisler et al. (1997). Neither of these studies reaches more than ~ 1 mag below the main-sequence turn-off (MSTO), and indeed in both, the turn-off is only measured at low signal-to-noise.

In this paper we take advantage of the existence of observations of ESO 121-SC03 taken with the Advanced Camera for Surveys (ACS) on *HST* as part of our recent snapshot survey of LMC and SMC star clusters (program 9891), to make deep, high quality photometric measurements of this cluster. Our resulting VI CMD reaches more than 3 magnitudes below the main-sequence turn-off, representing by far the deepest observations of ESO 121-SC03 to date. We use these data to conduct a detailed study of the age of ESO 121-SC03 relative to two comparison clusters – the young accreted Sagittarius dSph globular cluster Palomar 12 (also imaged with ACS in program 9891), and the old Galactic globular cluster 47 Tuc. We find that ESO 121-SC03 is significantly younger than 47 Tuc, but very similar in age to Pal. 12, confirming the earlier conclusion of Mateo et al. (1986) and Geisler et al. (1997) that ESO 121-SC03 does indeed lie squarely within the LMC cluster age-gap.

2 OBSERVATIONS AND DATA REDUCTION

The observations were taken during *HST* Cycle 12 using the ACS Wide Field Channel (WFC). As snapshot targets, the clusters were observed for only one orbit each. This allowed two exposures to be taken per cluster – one through the F555W filter and one through the F814W filter. Details of the individual exposures are listed in Table 1.

The ACS WFC consists of a mosaic of two 2048×4096 SITe CCDs with a scale of ~ 0.05 arcsec per pixel, and separated by a gap of ~ 50 pixels. Each image therefore covers a field of view (FOV) of approximately 202×202 arcseconds. The clusters were centred at the reference point WFC1, located on chip 1 at position (2072 , 1024). This allowed any given cluster to be observed up to a radius $r \sim 150''$ from its centre, while also ensuring the cluster core did not fall near the inter-chip gap.

Our observations were made with the ACS/WFC GAIN parameter set to 2. This allows the full well depth to be sampled (as opposed to only ~ 75 per cent of the full well depth for GAIN = 1) with only a modest increase in read noise (~ 0.3 e$^-$ extra rms), thus increasing the dynamic range of the observations by greater than 0.3 mag over that obtained with the default gain. In addition, we offset the second image of each cluster by 2 pixels in both the x and y directions, to help facilitate the removal of hot pixels and cosmic rays. With only two images per cluster, through different filters, it is not possible to completely eliminate the inter-chip gap using such an offset.

During retrieval from the STScI archive, all images were passed through the standard ACS/WFC reduction pipeline. This process includes bias and dark subtractions, flatfield division, masking of known bad pixels and columns, and the calculation of photometry header keywords. In the final stage of the pipeline, the PYRAF MULTIDRIZZLE software is used to correct the (significant) geometric distortion present in WFC images. The products obtained from the STScI archive are hence fully calibrated and distortion-corrected drizzled images, in units of counts per second.

For both clusters, we performed photometry on the F555W and F814W images individually, using the DAOPHOT software in IRAF. First the DAOFIND task was used with a detection threshold of 4σ above background to locate all the brightness peaks in each image. The two output lists were matched against each other to find objects falling at identical positions in the two frames. Objects detected in one image but with no matching counterpart in the other image were discarded. Because of the significant geometric distortion present in ACS/WFC images, a 2×2 pixel offset in telescope position does not correspond to a uniform 2×2 pixel offset between the two drizzled frames; in fact the offset is position dependent. To match between the two lists, we therefore transformed all measured positions into the coordinate systems of the original distorted flat-fielded images and matched between these new lists. For this transformation we employed the PYRAF task TRAN.

Next, we used the PHOT task to perform aperture photometry on all objects in the cross-matched lists, on each of the two images. For this we used an aperture radius of 4 pixels. This radius was selected after some experimentation, which demonstrated it to give the narrowest sequences on the two cluster CMDs. We also performed measurements using the recently developed DOLPHOT software (similar to HSTPHOT, described by Dolphin (2000)); however we found that our aperture photometry pipeline consistently returned narrower CMD sequences for our two clusters. We therefore selected the aperture photometry as our preferred measurements for the present study. It is important to note both ESO 121-SC03 and Pal. 12 are very sparse clusters, so crowding is not an issue in the ACS/WFC images, and aperture photometry is a perfectly acceptable technique. Comparing the offsets between our aperture photometry (after cleaning and the application of the corrections and zero-points described below) and the DOLPHOT measurements revealed mean magnitude-independent offsets of $\lesssim 0.01$ mag in both F555W and F814W. Hence we are confident in the accuracy of our photometric measurements.

We completed the photometric calibration using the results of Sirianni et al. (2005). Magnitudes were calculated in the ACS/WFC VEGAMAG system, defined as the system in which Vega has magnitude 0 in all filters. From Sirianni et al. (2005), the relevant zero-points for this system are 25.724 in F555W and 25.501 in F814W.

Like all previous *HST* CCD instruments, the

Table 1. ACS/WFC observations of ESO 121-SC03 and Pal. 12 (*HST* program 9891).

Cluster	RA (J2000.0)	Dec. (J2000.0)	Filter	Image Name	Exposure Time (s)	Date
ESO 121-SC03	$06^{\rm h}\ 02^{\rm m}\ 01.36^{\rm s}$	$-60^\circ\ 31'\ 22.6''$	F555W	j8ne79sdq	330	07/10/2003
			F814W	j8ne79smq	200	07/10/2003
Palomar 12	$21^{\rm h}\ 46^{\rm m}\ 39.18^{\rm s}$	$-21^\circ\ 15'\ 06.8''$	F555W	j8ne80koq	53	26/07/2003
			F814W	j8ne80kqq	32	26/07/2003

ACS/WFC chips are suffering from degradation of their charge transfer efficiency (CTE) due to radiation damage. This can cause position dependent errors in photometric measurements of up to ~ 10 per cent under certain circumstances (see Sirianni et al. (2005) and Riess & Mack (2004) for detailed discussions). To correct for the charge loss, we employed the calibration of Riess & Mack (2004), who provide a time-dependent parametrization of the necessary correction due to parallel (y-direction) transfers:

$$\Delta_Y = 10^A \times s^B \times f^C \times \frac{Y}{2048} \times \frac{(MJD - 52333)}{365} \ \text{mag} \quad (1)$$

for any given object. In this equation, the object's sky (s) and flux (f) values are in counts; Y represents the number of parallel transfers (so if the object has position (x, y) on either of the two ACS chips, then $Y = y$ for objects on chip 2, and $Y = 2048 - y$ for objects on chip 1); and MJD is the Modified Julian Date of the observation being corrected. The parameters A, B, and C are tabulated by Riess & Mack (2004) for three different apertures (3, 5, and 7 pixels). As our 4 pixel aperture has not been calibrated, we used the average of the corrections necessary for 3 and 5 pixel apertures. In the presently available calibration there is no requirement for corrections due to serial (x-direction) transfers.

Our final step was to apply aperture corrections to the photometry. For this, we followed the process described by Sirianni et al. (2005). For the F555W measurements, we selected a sub-sample of suitable stars (see below) and used the PHOT task to measure photometry with a $0.5''$ aperture (10 WFC pixels). This allowed the correction from our 4 pixel aperture to $0.5''$ to be calculated. We then applied the correction from a $0.5''$ aperture to an infinite aperture listed by Sirianni et al. (2005) (AC05 in their terminology, where AC05 = 0.092 mag in F555W). The procedure for F814W was more complicated, as in the near-IR ACS filters the aperture correction is a function of colour for red stars. This is due to the scattering of red light in the CCDs, which results in a broadened PSF and long-wavelength halo (Sirianni et al. 2005). We therefore used the CALCPHOT routine in SYNPHOT and the BPGS stellar atlas available in STSDAS to determine the relationship between the instrumental colour F555W-F814W of any given star and its effective wavelength, as described by Sirianni et al. Here, the effective wavelength is a parameter which represents the mean wavelength of detected photons:

$$\lambda_{\rm eff} = \frac{\int f_\lambda(\lambda) P(\lambda) \lambda^2 d\lambda}{\int f_\lambda(\lambda) P(\lambda) \lambda d\lambda}, \quad (2)$$

where $P(\lambda)$ is the passband transmission curve (F814W in our case), and $f_\lambda(\lambda)$ is the flux distribution of the object. Having defined this relationship, we estimated the effective wavelength of each detected star from the measured instrumental colour. A suitable subset of stars with blue effective wavelength[1] were used to calculate the aperture correction to $0.5''$, just as with the F555W measurements. This value, along with AC05 (equal to 0.087 in F814W) was applied for blue stars. For all redder stars (i.e., with $\lambda_{\rm eff} > 8200$Å), wavelength-dependent aperture corrections were applied directly from Table 6 of Sirianni et al. (2005).

In selecting suitable aperture stars, we applied the following criteria: they must be bright stars but significantly below saturation; they must not have unusual shape characteristics (see Section 3.1); they must have no neighbouring stars, bad pixels, cosmic rays, or image edges within a radius of $1''$; and they must not lie in an area of unusually high background (e.g., near a very bright star). In addition, for the F814W selection, they must have $\lambda_{\rm eff} \leqslant 8200$Å. For ESO 121-SC03, these defined a sample of 57 stars in F555W and 90 stars in F814W; while for Palomar 12 they defined samples of 231 and 210 stars respectively. The mean aperture correction to $0.5''$ was calculated for each image using a 3σ clipping algorithm. Standard errors in the calculated corrections were typically ~ 0.01 mag.

3 RESULTS

3.1 Colour-magnitude diagrams

We present the final colour-magnitude diagrams (CMDs) for ESO 121-SC03 and Pal. 12 in Fig. 1. Both stellar samples have been cleaned using the PSF shape parameters (e.g., sharpness, roundness) obtained during the photometric measurement process. This filtering is necessary to help remove cosmic rays and other spurious or non-stellar detections. Because of the nature of the snapshot observations, only one image was taken in each filter; hence more cosmic rays propagate through the photometry pipeline than in the usual scenario where multiple images per passband are median filtered prior to the photometric measurements in order to remove spurious objects.

To apply the quality filter we used the three shape characteristics from DAOFIND: one sharpness and two roundness parameters. The sharpness is a measurement of how high the peak of a detection is relative to a best-fitting Gaussian, while the two roundness parameters are measurements

[1] Specifically, stars with $\lambda_{\rm eff} \leqslant 8200$Å. In practice, the bluest stars have $\lambda_{\rm eff} \sim 8000$Å in F814W.

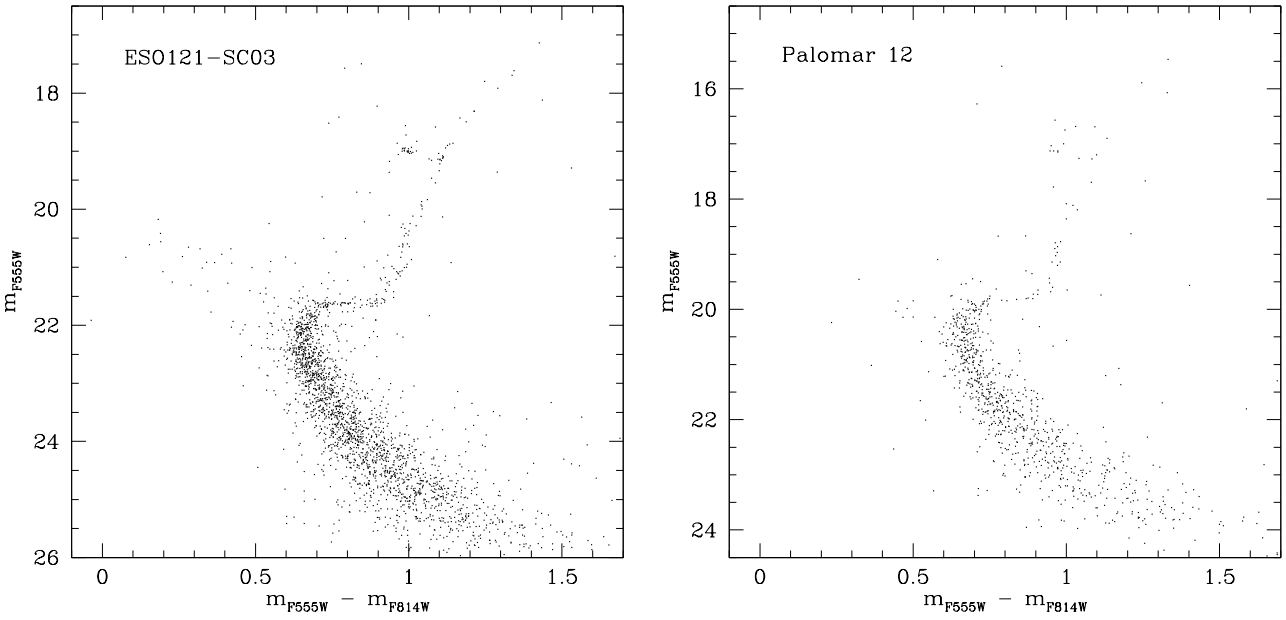

Figure 1. Cleaned colour-magnitude diagrams for ESO 121-SC03 and Palomar 12. Measurements are plotted in the VEGAMAG magnitude system (see text). The CMD for ESO 121-SC03 contains 2 386 detections, while that for Palomar 12 contains 944 detections.

of how circular an object is. Clean stellar detections should have sharpness ~ 0.75 and roundness ~ 0. For both photometry lists we produced histograms of the three relevant parameters to determine suitable clipping limits. Because both targets are sparse clusters, we set rather lenient limits in order to maintain clear CMD sequences. For both, we only retained objects with $0.6 \leqslant$ sharpness $\leqslant 0.9$ and objects with $-0.5 \leqslant$ roundness $\leqslant 0.5$ through each passband. This typically removed about ~ 30 per cent of detections, predominantly at the faintest magnitudes.

We did not apply any filtering to remove field star contamination, as both clusters are set against sparse fields – ESO 121-SC03 is projected $\sim 10^\circ$ from the optical centre of the LMC, while Pal. 12 lies at a Galactic latitude of almost -50°. The observed field of view is not sufficiently large to make an accurate estimate of the surface density of field stars, in order to make an accurate subtraction.

The CMDs for both clusters show stubby red horizontal branches, consistent with previous studies (e.g., Mateo et al. 1986; Rosenberg et al. 1998). Both CMDs also show populations of blue straggler candidates. It is already known that Pal. 12 possesses such objects (e.g., Rosenberg et al. 1998); however we know of no discussion of blue stragglers in ESO 121-SC03. We discuss the blue straggler population of this cluster in more detail below (Section 3.4).

Our CMD for ESO 121-SC03 reaches ~ 3 mag below the main-sequence turn-off, as does that for Pal. 12. This is the highest quality published CMD for ESO 121-SC03, and offers the opportunity for an accurate relative age measurement. While we would prefer to work in the native ACS photometric system to perform such a measurement, we could not locate suitably sampled stellar isochrones (which we require in order to establish the relative age calibration) calculated in this system. We therefore used the relations derived by Sirianni et al. (2005) to transform our photometry into standard Johnson-Cousins V and I magnitudes. These relations take the form of an iterative transformation:

$$\mathrm{TMAG} = \mathrm{SMAG} + c_0 + (c_1 \times \mathrm{TCOL}) + (c_2 \times \mathrm{TCOL}^2) \quad (3)$$

where the target magnitude and colour are TMAG and TCOL respectively, the source magnitude is SMAG, and c_0, c_1 and c_2 are the transformation coefficients listed in Table 22 of Sirianni et al. (2005). To apply the transformation for a given star, we first subtract the VEGAMAG zeropoints to obtain SMAG in F555W and F814W. This also yields the source colour F555W-F814W, which we adopt as a crude first estimate of TCOL. Using the appropriate coefficients in Eq. 3 then provides first estimates of TMAG in V and I. These in turn give an improved estimate of TCOL, and the procedure is iterated until convergence.

Fig. 2 presents the CMDs for ESO 121-SC03 and Pal. 12 in the standard Johnson-Cousins photometric system. By comparing these to the CMDs in Fig. 1 it is clear that the transformations have not drastically reshaped the colour-magnitude plane. This observation, along with the fact that Sirianni et al's transformations were derived using a Galactic globular cluster[2] leads us to have confidence that we have not introduced damaging systematic errors into our photometry. We verify this more explicitly in Section 3.2, below.

3.2 Photometric metallicities and reddenings

Although a number of metallicity estimates already exist for both ESO 121-SC03 and Pal. 12, our new observations provide an opportunity to add additional measurements. Mak-

[2] i.e., a stellar population not very different to those examined here – although admittedly the cluster in question (NGC 2419) is ~ 1 dex more metal poor than either ESO 121-SC03 or Pal. 12.

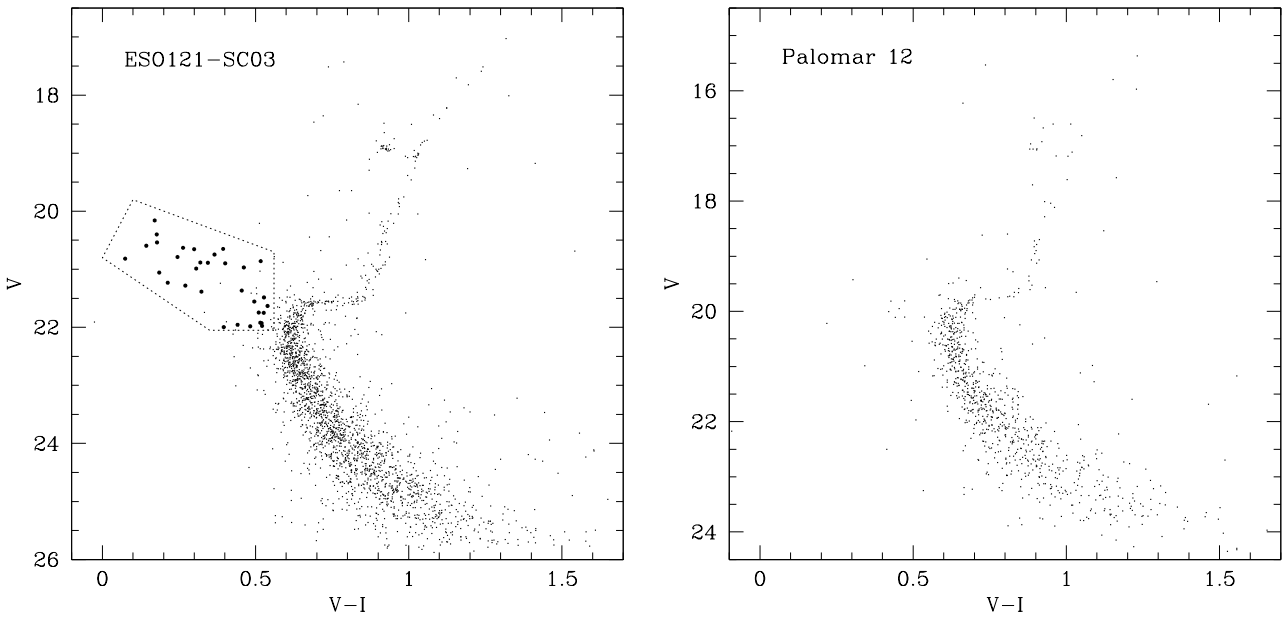

Figure 2. Cleaned colour-magnitude diagrams for ESO 121-SC03 and Palomar 12, where the photometry has been transformed from the VEGAMAG system to Johnson-Cousins V and I according to the prescription of Sirianni et al. (2005) (see also text). On the CMD for ESO 121-SC03 we have marked a region defining the blue straggler population for this cluster. As described in the text, 40 stars lie in this region, 32 of which are very clean stars on the ACS images (bold points).

ing these also allows us to check the consistency of our transformed photometry. We employ the calibration of Sarajedini (1994), who used high quality observations of six Galactic globular clusters to derive a method of simultaneously estimating the reddening and metallicity of a cluster from its (V, $V-I$) CMD. His method relies on the measurement of the level of the horizontal branch (HB) and the colour of the red-giant branch (RGB) at the HB level, together with some parametrization of the RGB fiducial above the HB level. The calibration then relates the height of the RGB above the HB at intrinsic colour $(V-I)_0 = 1.2$ to the metallicity (this parameter is labelled $\Delta V_{1.2}$), and the measured colour of the RGB at $V_{\rm HB}$ (labelled $(V-I)_g$) to the reddening.

We chose to adopt the common procedure of fitting a second order polynomial to the upper RGB of the cluster under consideration, so that it is parametrized by $(V-I) = a_0 + a_1 V + a_2 V^2$. We fit this relation iteratively, discarding outlying points on each loop. The results may be seen for ESO 121-SC03 and Pal. 12 in Fig. 3 and Table 2. Both clusters (but particularly Pal. 12) are sparse, so their upper RGBs are not very well defined. This means that the resulting parametrizations are correspondingly uncertain.

Fig. 3 and Table 2 also display the calculated HB levels. In both clusters the HBs are narrow and short, so the HB levels are well defined and straightforward to measure. We find $V_{\rm HB} = 18.90 \pm 0.03$ for ESO 121-SC03, and $V_{\rm HB} = 17.05 \pm 0.03$ for Pal. 12. These values compare reasonably well with those found in previous studies. For example, Mateo et al. (1986) measured $V_{\rm HB} = 19.0$ for ESO 121-SC03, while Sarajedini et al. (1995) calculated $V_{\rm HB} = 18.96$ from the same photometry. Similarly, Stetson et al. (1989) measured $V_{\rm HB} = 17.13$ for Pal. 12, while Sarajedini et al. (1995) found $V_{\rm HB} = 17.10$, again from the same data. Gratton & Ortolani (1988) obtained $V_{\rm HB} = 17.05 \pm 0.02$ for Pal. 12, and more recently Rosenberg et al. (1998) measured $V_{\rm HB} = 17.18$ for this cluster, although they found that their photometric calibration in the V-band was on average 0.12 mag fainter than that of Gratton & Ortolani (1988), and 0.05 mag fainter than that of Stetson et al. (1989). There is a tendency for our measurements to be ~ 0.05 mag brighter than the literature values. It is not clear whether this is a systematic offset or whether it simply represents random observational errors. Nonetheless, the consistency between our aperture photometry and that derived using DOLPHOT (see Section 2), as well as our measurements of 47 Tuc (see Section 4, below) leads us to have confidence in our photometry. For the most part, any such small global offsets will in any case be irrelevant, since from here on we mostly consider differential measures on the CMD (e.g., the difference between $V_{\rm HB}$ and the main-sequence turn-off level as an age indicator).

Applying Sarajedini's (1994) method, we obtained metallicity and reddening measurements of [Fe/H] $= -0.97 \pm 0.10$ and $E(V-I) = 0.04 \pm 0.02$ for ESO 121-SC03, and [Fe/H] $= -1.05 \pm 0.10$ and $E(V-I) = 0.00 \pm 0.02$ for Pal. 12. These are recorded in Table 2.

Our measurements for ESO 121-SC03 are in good agreement with previous results. Mateo et al. (1986) concluded [Fe/H] $= -0.9 \pm 0.2$ for this cluster from their (B, $B-V$) CMD, while Olszewski et al. (1991) measured [Fe/H] $= -0.93 \pm 0.1$ spectroscopically and Bica et al. (1998) derived [Fe/H] $= -1.05 \pm 0.2$ from Washington photometry. More recently, Hill et al. (2000) obtained [Fe/H] $= -0.91 \pm 0.16$ from high resolution spectroscopic measurements made with VLT/UVES. There are fewer estimates of the foreground reddening for ESO 121-SC03. Both Mateo et al.

Table 2. Results of the simultaneous determination of cluster reddenings and metallicities.

Cluster	$V_{\rm HB}$	a_0	a_1	a_2	$\Delta V_{1.2}$	[Fe/H]	$E(V-I)$
ESO 121-SC03	18.90 ± 0.03	19.60150	−1.87403	0.04719	1.31 ± 0.10	-0.97 ± 0.10	0.04 ± 0.02
Palomar 12	17.05 ± 0.03	16.84290	−1.78086	0.04991	1.40 ± 0.10	-1.05 ± 0.10	0.00 ± 0.02

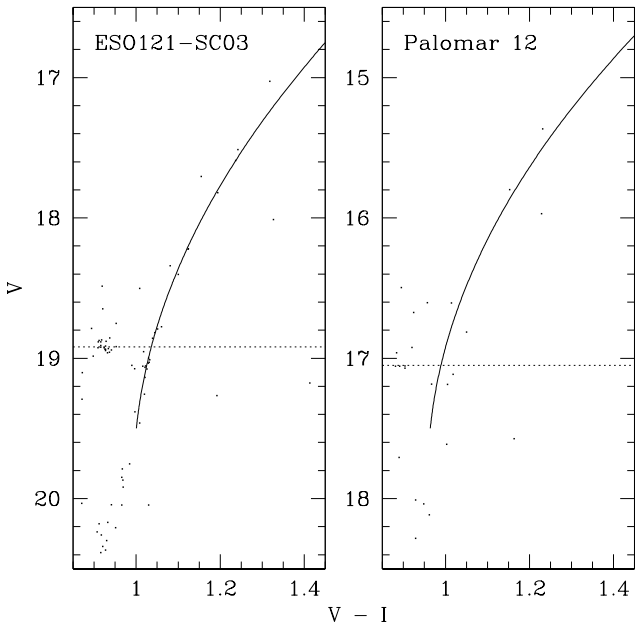

Figure 3. Quadratic fits to the two cluster RGBs, used for the reddening and metallicity estimates. The dotted lines indicate the HB levels. Note that the brightest star in the ESO 121-SC03 red-giant branch (at $V \sim 17$) was not included in the fit for this cluster as it is saturated in the F814W image and hence has large colour uncertainty.

(1986) and Bica et al. (1998) adopt $E(B-V) = 0.03$ from the Burstein & Heiles (1982) maps, which corresponds to $E(V-I) \sim 0.04$ if we use the relation that $E(V-I) = 1.31E(B-V)$ (see e.g., Mackey & Gilmore 2003b). For comparison, the Schlegel et al. (1998) dust maps give a value of $E(B-V) = 0.04$, which is also consistent with our measurement. The close agreement between our present results and those in the literature suggests that we have not introduced any significant systematic errors into our photometry by transforming out of the native ACS/WFC photometric system.

For Pal. 12, a number of previous metallicity estimates exist. As summarized by Rosenberg et al. (1998), Da Costa & Armandroff (1990) determined [Fe/H] $= -1.06 \pm 0.12$ from VI photometry, while Armandroff & Da Costa (1991) measured [Fe/H] $= -0.60 \pm 0.14$ spectroscopically, and Da Costa & Armandroff (1995) found [Fe/H] $= -0.64 \pm 0.09$ from a re-analysis of the same data. Brown et al. (1997) conducted a higher resolution spectroscopic study of two Pal. 12 giants, obtaining [Fe/H] $= -1.0 \pm 0.1$, and Rosenberg et al. (1998) themselves measured [Fe/H] $\simeq -0.93$ from VI photometry. Most recently, Cohen (2004) has measured [Fe/H] $\simeq -0.8$ from high resolution Keck spectra of four Pal. 12 giants. For the reddening towards this cluster, Rosenberg et al. (1998) assume $E(V-I) = 0.03$ based on several earlier measurements, while the Schlegel et al. (1998) maps imply $E(V-I) \simeq 0.05$. Harris (1996, 2003 update) lists $E(B-V) = 0.02$, which corresponds to $E(V-I) \simeq 0.03$.

Our measured metallicity and reddening for Pal. 12 do not agree as closely with previous measurements as our results for ESO 121-SC03 do; however we feel that this is most likely due to the poor definition of the Pal. 12 RGB on our CMD rather than any large systematic error in the photometry. Pal. 12 is a sparse, diffuse cluster, and this is compounded by the relatively small ACS/WFC field of view – Rosenberg et al. (1998) find a tidal radius of $r_t \sim 7.6'$, compared with the $\sim 3.3' \times 3.3'$ ACS/WFC field of view. Hence we have few stars with which to determine the RGB fiducial. In particular, Fig. 3 shows that the uncertainty in the colour of the RGB at the HB level is relatively large, which explains the small discrepancy between our foreground reddening estimate and those in the literature. Similarly, the upper RGB is effectively defined by only two stars, which introduces a corresponding uncertainty into our metallicity estimate.

Given the above results and discussion, we will adopt [Fe/H] $= -0.95 \pm 0.05$ and $E(V-I) = 0.04 \pm 0.02$ for ESO 121-SC03 for the remainder of this paper. For Pal. 12 we will assume [Fe/H] $= -0.80 \pm 0.10$ based on the recent high quality spectra of Cohen (2004)[3], along with a colour excess $E(V-I) = 0.03 \pm 0.02$.

3.3 Distance of ESO 121-SC03

It is worth briefly considering the distance of ESO 121-SC03, both from us and from the centre of the LMC. In the previous Section we measured the HB level for this cluster to be $V_{\rm HB} = 18.90 \pm 0.03$. We also estimated a colour excess $E(V-I) = 0.04 \pm 0.02$, which corresponds to a V-band extinction $A_V = 0.095 \pm 0.047$. To determine the distance modulus, we must adopt some relationship between metallicity and the intrinsic luminosity of the HB. Chaboyer (1999) concluded that

$$M_V({\rm HB}) = (0.23 \pm 0.04)([{\rm Fe/H}] + 1.6) + (0.56 \pm 0.12) \ , \quad (4)$$

while Gratton et al. (2003) found that

$$M_V({\rm HB}) = (0.22 \pm 0.05)([{\rm Fe/H}] + 1.5) + (0.56 \pm 0.07) \ , \quad (5)$$

[3] We note that the mean of the six literature measurements discussed above, plus our own for this cluster is [Fe/H] $= -0.84$, in good agreement with the Cohen (2004) measurement.

from their detailed study of the globular clusters NGC 6397, NGC 6752 and 47 Tuc. Taking the mean of the two values of M_V(HB) so calculated for ESO 121-SC03 (with [Fe/H] $= -0.95 \pm 0.05$), we find M_V(HB) $= 0.695 \pm 0.010$ for this cluster (where the quoted error is due only to our random error in [Fe/H]). In combination with our measured HB level and V-band extinction this implies a distance modulus $\mu = 18.11 \pm 0.09$. This is significantly shorter than the standard LMC distance modulus $\mu_{\rm LMC} = 18.50 \pm 0.09$ (see e.g., Gratton et al. 2003, and references therein). In terms of linear distance, ESO 121-SC03 is ~ 20 per cent closer to us than is the LMC.

This result suggests that ESO 121-SC03 is located further away from the centre of the LMC than its projected angular separation would imply. Adopting the optical centre of the LMC from Bica et al. (1996), at $\alpha = 05^{\rm h}\,20^{\rm m}\,56^{\rm s}$, $\delta = -69^\circ\,28'\,41''$, ESO 121-SC03 lies at a projected angular separation of 9.9°. Assuming the two distance moduli quoted above leads to the conclusion that the linear distance between the centre of the LMC and ESO 121-SC03 is close to 11.5 kpc. This renders ESO 121-SC03 one of the most remote known LMC star clusters.

3.4 Blue stragglers in ESO 121-SC03

As noted above, our CMD for ESO 121-SC03 shows the population of blue straggler candidates to be rather large, including a significant number of very blue objects. Since we know of no prior discussion of blue stragglers in ESO 121-SC03, we examined this population in more detail.

In Fig. 2 we have selected blue straggler candidates by defining a region on the CMD which encompasses them. The number of stars falling within this region is 40. We examined each star by eye on our F555W and F814W ACS/WFC images of ESO 121-SC03, and eliminated all stars which showed some hint of being affected by blends or cosmic ray strikes. This reduced the sample to 32 stars. These are marked in bold on Fig. 2. Clearly, the large and extended blue straggler population remains, so we are confident that our photometry for these stars is good.

Since we have not made any attempt to remove field stars from our CMD, we would like to rule out the possibility of significant contamination by such objects. We therefore calculated the projected radius of each candidate blue straggler from the cluster centre, and constructed a cumulative distribution of the number of blue stragglers with projected radius. This may be seen in the upper panel of Fig. 4. In this plot, the two dashed lines represent the cumulative distributions for our original sample of 40 stars and our cleaned sample of 32. The two solid lines show the expected cumulative distribution with radius of a uniform background stellar population with a surface density normalized to match the observed number of blue straggler candidates within the maximum radius (either 40 or 32). Note that in constructing these two comparison lines, we have accounted for the ACS/WFC field-of-view – hence the deviation from a pure R^2 function visible at larger radii. From this plot, it is clear that the blue straggler candidates are far more centrally concentrated than a uniformly distributed background, which strongly suggests they are cluster members rather than field stars.

In the lower panel of Fig. 4 we compare the radial distribution of blue stragglers with that of main sequence stars in ESO 121-SC03. We selected our main sequence sample by taking all stars below the main-sequence turn-off (at $V = 22.16$ – see Section 4.2), above the approximate faint detection limit (at $V \sim 26$), and within 3σ of the approximate main-sequence ridge-line. This sample does not represent all main-sequence stars, since our photometry is not deep enough to reach very low-mass objects; but is representative of the most massive present-day main sequence members. The cumulative distributions of these stars, normalized to our two blue straggler sample sizes, are plotted as the solid lines in the lower panel of Fig. 4. Clearly the blue straggler candidates are significantly more centrally concentrated than the main sequence stars. As demonstrated below, this observation is consistent with dynamical mass segregation having occurred in ESO 121-SC03.

Piotto et al. (2004) examined blue straggler relative frequency $F_{\rm BSS}$ as a function of integrated cluster luminosity M_V and of central luminosity density ρ_0 for a large sample of Galactic globular clusters observed with *HST*. They found a significant anti-correlation between $F_{\rm BSS}$ and M_V, and also between $F_{\rm BSS}$ and ρ_0 for $\log \rho_0 < 3.2$ (see their

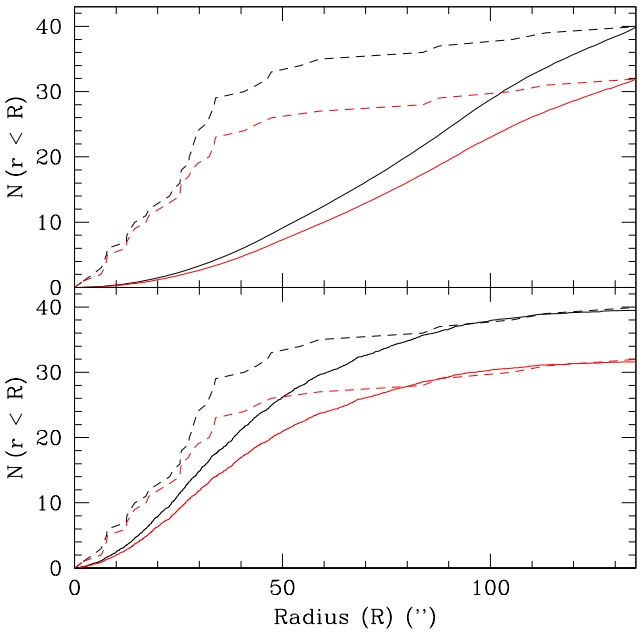

Figure 4. Cumulative distributions of blue straggler candidates with projected radius. In both panels, the dashed lines represent the observed distributions for our cleaned sample of 32 (lower line) and our original sample of 40 (upper line). In the upper panel, for comparison we have also plotted the expected distributions for a uniformly distributed background with surface density normalized as described in the text (solid lines). Clearly our blue straggler candidates are associated with the cluster rather than a uniform field star population. The abrupt flattening in the blue straggler distributions beyond $\sim 50''$ is at least partly due to the restricted ACS/WFC field of view. This flattening is also visible in the solid lines, which deviate from a pure R^2 relation at large radii. In the lower panel the solid lines represent the radial distribution of upper main sequence stars (see text). The blue straggler population is clearly more centrally concentrated than these main sequence objects.

Table 3. ACS/WFC observations of 47 Tuc (Program 9018).

Cluster	RA (J2000.0)	Dec. (J2000.0)	Filter	Image Name	Exposure Time (s)	Date
47 Tuc (pair 1)	$00^{\rm h}\ 22^{\rm m}\ 37.20^{\rm s}$	$-72^\circ\ 04'\ 14.0''$	F555W	j8c0b1tzq	30	09/05/2002
			F814W	j8c0d1caq	30	06/05/2002
47 Tuc (pair 2)	$00^{\rm h}\ 22^{\rm m}\ 37.20^{\rm s}$	$-72^\circ\ 04'\ 14.0''$	F555W	j8c0b1u1q	30	09/05/2002
			F814W	j8c0d1ccq	30	06/05/2002
47 Tuc (pair 3)	$00^{\rm h}\ 22^{\rm m}\ 37.20^{\rm s}$	$-72^\circ\ 04'\ 14.0''$	F555W	j8c0b1skq	30	09/05/2002
			F814W	j8c032xuq	5	19/04/2002

Figure 1). It is instructive to consider where ESO 121-SC03 lies with regard to these anti-correlations. $F_{\rm BSS}$ is defined in Piotto et al. (2004) as the number of blue stragglers normalized to the number of horizontal branch stars. For ESO 121-SC03, we observe $N_{\rm HB} = 19$ from Fig. 2. If we then assume a population $N_{\rm BSS} = 36 \pm 4$, we find $F_{\rm BSS} = 1.9 \pm 0.2$, i.e., $\log F_{\rm BSS} \approx 0.3$.

Adopting the best fitting structural parameters of Mateo et al. (1986), who found a central surface brightness $\sigma_{V,0} = 22.3$, a core radius $r_c = 34''$ and tidal radius $r_t = 136''$ for ESO 121-SC03, we estimate $\log \rho_0 \approx 0.7$ for this cluster according to the prescription of Djorgovski (1993). Mateo et al. (1986) also obtained the apparent integrated magnitude of ESO 121-SC03, $V_{\rm ESO} = 13.4$, which at our distance modulus and assumed reddening corresponds to $M_V \approx -4.8$. From examination of Figure 1 in Piotto et al. (2004), we see that ESO 121-SC03 falls at much lower $\log \rho_0$ and M_V than do any of the Galactic globular clusters in their sample. It also has a higher $F_{\rm BSS}$ than all but two of the clusters in their sample. Hence our observations for ESO 121-SC03 are consistent with, and significantly extend the anti-correlations observed by these authors.

Since stellar collisions are clearly not frequent in as low a density cluster as ESO 121-SC03, the observed population of blue stragglers is presumably linked to the evolution of primordial binary stars in this cluster. Mateo et al. (1986) measure the half-mass radius of ESO 121-SC03 to be $r_h = 38''$. Adopting a mean stellar mass of $0.33 M_\odot$ and a global mass-to-light ratio $M/L \sim 2$, we calculate a median relaxation time for ESO 121-SC03 of $t_{rh} \sim 1.6$ Gyr, using the prescription of Eq. 8-72 in Binney & Tremaine (1987). Since dynamical mass segregation occurs on approximately the two-body relaxation time-scale, our observation that the blue stragglers are more centrally concentrated than the most massive main sequence stars in ESO 121-SC03 is consistent with dynamical mass segregation having occurred in this cluster, and with the likelihood that the observed population of blue stragglers is linked to the evolution of primordial binary stars.

4 RELATIVE AGE MEASUREMENTS

As described in Section 1, ESO 121-SC03 has been shown by several studies to be a few Gyr younger than the oldest clusters in the LMC. The availability of our high quality ACS photometry offers the opportunity to place the tightest constraints yet on the age of this cluster. The most precise way to do this is to obtain an age estimate relative to other globular clusters for which well determined measurements already exist. One such cluster is Pal. 12, which is why we have included it in the present study. As discussed previously, this cluster has been demonstrated by a number of authors to be considerably younger than the oldest Galactic globular clusters, just as ESO 121-SC03 is younger than the oldest LMC objects. For example, Rosenberg et al. (1998) found Pal. 12 to have an age of only 68 ± 10 per cent that of 47 Tuc and M5.

Ideally, we would like to also include an older globular cluster than ESO 121-SC03 in the relative age measurements. Only one such cluster, of similar metallicity to ESO 121-SC03, has been observed with ACS/WFC in the F555W and F814W filters. This is 47 Tuc (NGC 104), with [Fe/H] $= -0.76$ (Harris 1996). In order to include this object in our present study, we obtained suitable imaging from the HST archive (taken as part of the ACS calibration program 9018) and reduced it using exactly the same photometric pipeline (described in Section 2) that we used for ESO 121-SC03 and Pal. 12. The three pairs of specific images we used, and their exposure durations, are listed in Table 3. Note that these observations are centred on a field located $\sim 6.8'$ from the nominal cluster centre (which is at $00^{\rm h}\ 24^{\rm m}\ 05.2^{\rm s}$, $-72^\circ\ 04'\ 51.0''$). This offset helped ameliorate any crowding issues associated with observing near the centre of this object.

At the end of the photometric reduction we were left with three CMDs from the three pairs of observations. We matched stellar coordinates between these lists, keeping only objects appearing in all three. The measured magnitudes were combined in an error weighted mean to obtain the final photometric measurements. The final, transformed CMD may be seen in Fig. 5, consisting of a long, narrow main sequence and very well defined turn-off region. Unfortunately, because of the image exposure durations, all stars brighter than $V \sim 15.5$ are very saturated and could not be measured accurately. No shorter duration images are available in the archive, so we could not obtain a CMD including the HB. Nevertheless, this incompleteness did not compromise our age measurements. As discussed below, 47 Tuc is a very well studied cluster and it is possible to obtain good estimates of the HB level from the literature.

4.1 Theoretical calibration

For our relative age measurements, we used two techniques – the so-called vertical and horizontal methods. Both employ differential indicators on the CMD. The vertical method

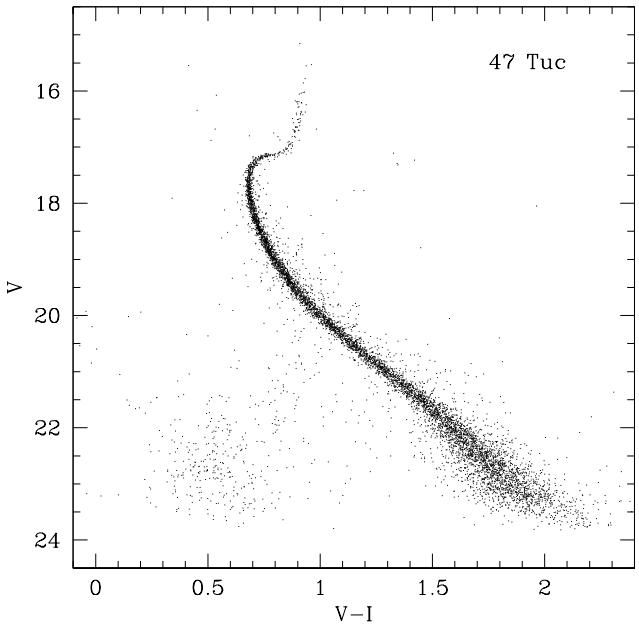

Figure 5. Cleaned VI colour-magnitude diagram for 47 Tuc. As described in the text, these measurements are derived from observations of a field offset from the cluster centre by $\sim 6.8'$. The non-cluster population evident around $(V, V-I) = (23, 0.5)$ are background SMC field stars.

relies on the fact that the difference between the level of the HB ($V_{\rm HB}$) and the level of the MSTO ($V_{\rm TO}$) is age-dependent, with older clusters having a larger value of this parameter. Similarly, the horizontal method makes use of the difference in colour between the MSTO and some point on the RGB below the HB. This relies on the fact that older clusters generally have shorter sub-giant branches (SGBs) and hence bluer RGBs below the HB.

Both the vertical and horizontal age dating techniques have some metallicity dependence which must be accounted for, which is one reason why we have selected reference clusters of similar metallicity to ESO 121-SC03. There is also some dependence on the abundance of α-process elements (e.g., O, Mg, Si, Ca, and Ti), which we would like to account for. It is well known that many Galactic globular clusters are enhanced in α-process elements relative to the solar value, with [α/Fe] $\sim +0.3$. A similar over-abundance has been observed for some old LMC clusters (see e.g., Johnson et al. 2004; Puzia et al. 2005). However, we know of only one relevant measurement for ESO 121-SC03 – that of Hill et al. (2000), who observed [O/Fe] $= +0.15$ in two red giants from high resolution spectra. These authors also measured [Al/Fe] in their two giants, and from the low observed abundance (~ -0.4) suggest that deep mixing has not occurred and therefore that the observed oxygen abundance is genuinely lower than that in comparable Galactic globular cluster giants, which typically have [O/Fe] $\sim +0.3 - 0.4$.

Apart from this measurement, the α-abundance of ESO 121-SC03 remains essentially unknown. Fortunately, our reference clusters span the range of [α/Fe] within which ESO 121-SC03 is likely to lie, as indicated by the observed value of [O/Fe]. 47 Tuc possesses the enhancement typical of many Galactic globulars – for example, from Carney (1996) we infer [α/Fe] $\simeq 0.18$ for this cluster, while Gratton et al. (2003) list [α/Fe] $= 0.30 \pm 0.02$. On the other hand, Pal. 12 shows no such enhancement – as demonstrated by the spectroscopic studies of Brown et al. (1997) and Cohen (2004), the latter of who found the mean of [Si/Fe], [Ca/Fe], and [Ti/Fe] to be -0.07 ± 0.05. Indeed, this pattern is one of the strongest clues linking Pal. 12 with the Sagittarius dwarf galaxy (Cohen 2004).

In order to establish a theoretical calibration against which to judge the relative ages of our three clusters, we used the recently published Victoria-Regina stellar models. For full details of these, see VandenBerg et al. (2006) and the references therein. The set of models most relevant to us consists of 60 grids of stellar evolutionary tracks – at each of 20 [Fe/H] values between -2.31 and the solar metallicity, for three [α/Fe] values (0.0, +0.3, and +0.6) per given iron abundance. For each grid, isochrones may be interpolated in $UBVRI$ for ages between 1 and 18 Gyr. Also provided are zero-age HB models which may be transformed to the observational plane at each [Fe/H] and [α/Fe] point.

For the present study we selected the grids constituting the four possible combinations of [Fe/H] $= -0.83$ and -1.01, and [α/Fe] $= 0.0$ and $+0.3$. These cover the range appropriate for the clusters in our present study. We interpolated V, $V-I$ isochrones from each grid for ages between 6 and 17 Gyr, at 0.5 Gyr intervals. On each isochrone we measured values of our vertical method and horizontal method indicators. For the vertical method we chose to use the difference in V magnitude between the level of the MSTO and the level of the HB, labelled $\Delta V_{\rm TO}^{\rm HB}$, while for the horizontal method we used $\delta(V-I)_{2.2}$ – the $V-I$ colour difference between the MSTO and the point on the RGB 2.2 mag brighter (in V) than the level of the MSTO. The exact point chosen on the RGB does not matter, as long as it is not too close to the SGB or the level of the HB (see e.g., Rosenberg et al. 1998). For the present work we chose the 2.2 mag level so as to be near to the brightest RGB stars in the CMD for 47 Tuc, without incorporating saturated objects.

To find the MSTO on each isochrone, we fit a second-order polynomial to the ~ 10 model points near the TO, and found its turning point. With this computed, it was straightforward to measure the colour of the RGB at $V_{2.2} = V_{\rm TO} - 2.2$ and determine $V_{\rm HB}$ from the appropriate ZAHB model. From these measurements we calibrated our relative age indicators as a function of [Fe/H] and [α/Fe]. The results may be seen in Fig. 6. In order to allow accurate relative age determinations for our three clusters, we fit third-order polynomials to the measured theoretical calibrations. The best-fitting polynomials are also drawn in Fig. 6, and their coefficients are listed in Table 4. These are defined by parametrizing the relationship between age, τ, and observed indicator, δ, by $\tau = b_0 + b_1\delta + b_2\delta^2 + b_3\delta^3$.

From Fig. 6, it can be seen that the vertical indicator $\Delta V_{\rm TO}^{\rm HB}$ is relatively insensitive to changes in [Fe/H] and [α/Fe] over the ranges spanned by our clusters. The greatest change in derived age for measured $\Delta V_{\rm TO}^{\rm HB}$ occurs with [Fe/H] at [α/Fe] $= 0.0$. In this case, $\Delta\tau \simeq 0.5 - 1$ Gyr moving from [Fe/H] $= -0.83$ to [Fe/H] $= -1.01$. The horizontal indicator exhibits far greater variance, particularly with [α/Fe] at given [Fe/H]. For example, at [Fe/H] $= -1.01$,

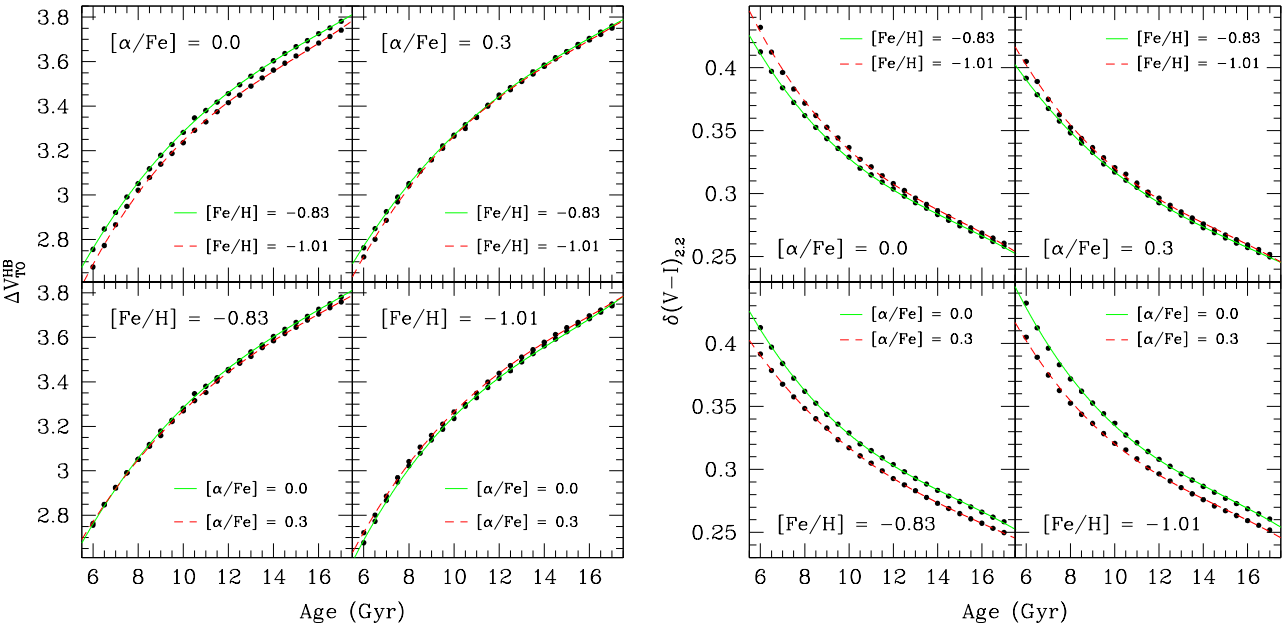

Figure 6. Theoretical age calibrations for our vertical method (left) and horizontal method (right) indicators, showing the variation with metallicity and α-enhancement (solid points). Selected metallicities are [Fe/H] = −0.83 and −1.01, each with [α/Fe] = 0.0 and +0.3. The green (solid) and red (dashed) lines represent the third-order polynomial fits, as described in the text.

Table 4. Vertical and horizontal method age calibration coefficients.

Method	[Fe/H]	[α/Fe]	b_0	b_1	b_2	b_3
Vertical	−0.832	+0.00	−63.2574	67.7981	−24.0045	3.09148
Vertical	−1.009	+0.00	−5.40693	14.9235	−7.98562	1.49592
Vertical	−0.832	+0.30	−70.1512	73.6266	−25.7156	3.27090
Vertical	−1.009	+0.30	−56.1248	63.0419	−23.1402	3.07405
Horizontal	−0.832	+0.00	103.963	−600.912	1261.43	−922.159
Horizontal	−1.009	+0.00	100.151	−569.686	1185.40	−859.686
Horizontal	−0.832	+0.30	111.519	−700.206	1619.40	−1327.04
Horizontal	−1.009	+0.30	98.2591	−565.779	1178.87	−850.567

moving from [α/Fe] = 0.0 to [α/Fe] = +0.3 leads to a reduction in the age of $\sim 10-15$ per cent.

Given these observations and the dearth of high resolution spectral measurements of stars in ESO 121-SC03, we decided it prudent to consider both the case where this cluster has [α/Fe] $\simeq$ 0.0 and the case where it has [α/Fe] $\simeq$ +0.3.

4.2 Results: vertical method

On each of the three cluster CMDs, we determined the colour and level of the MSTO by fitting a second-order polynomial to the data in this region, and finding the turning point of the fit. The results are listed in Table 5. We estimate our measured values of $V_{\rm TO}$ are accurate to ~ 0.05 mag, while those for $(V-I)_{\rm TO}$ are accurate to ~ 0.005 mag.

To calculate the vertical age indicator $\Delta V_{\rm TO}^{\rm HB}$, for ESO 121-SC03 and Pal. 12 we adopted $V_{\rm HB}$ as measured in Section 3.2. We are confident that these values are close indicators of the ZAHB level in these two clusters – for example, Recio-Blanco et al. (2005) recommend adopting the level 3σ above the lower envelope of the HB for clusters more metal-rich than [Fe/H] = −1, where σ is the typical error in V at the HB magnitude.

For 47 Tuc we do not have photometry of the HB region, so we searched the literature for recent accurate measurements of the HB level in this cluster. In their recent relative age study of 55 Galactic globular clusters, De Angeli et al. (2005) measured $V_{\rm HB}$ for 47 Tuc from both ground-based and HST/WFPC2 imaging, using the prescription of Recio-Blanco et al. (2005). They determined $V_{\rm HB} = 14.10 \pm 0.03$, which is the value we adopt for the present work. We are confident their photometry is on a very similar scale to ours for 47 Tuc, as they also measured $V_{\rm TO} = 17.65 \pm 0.08$, which is almost identical to our value. We note that Harris (1996) lists $V_{\rm HB} = 14.06 \pm 0.10$ for 47 Tuc, consistent with the measurement adopted here.

Next, we applied our theoretical age calibration to the measured values of $\Delta V_{\rm TO}^{\rm HB}$ to determine relative ages for the

Table 5. Observed vertical and horizontal relative age indicators for ESO 121-SC03, Pal. 12, and 47 Tuc.

Cluster	$V_{\rm TO}$	$(V-I)_{\rm TO}$	$V_{\rm HB}$	$\Delta V_{\rm TO}^{\rm HB}$	$(V-I)_{2.2}$	$\delta(V-I)_{2.2}$
ESO 121-SC03	22.16 ± 0.05	0.606 ± 0.005	18.90 ± 0.03	3.26 ± 0.06	0.941 ± 0.005	0.336 ± 0.007
Palomar 12	20.37 ± 0.05	0.613 ± 0.005	17.05 ± 0.03	3.32 ± 0.06	0.929 ± 0.005	0.317 ± 0.007
47 Tuc	17.66 ± 0.05	0.681 ± 0.005	14.10 ± 0.03	3.56 ± 0.06	0.960 ± 0.005	0.279 ± 0.007

Table 6. Relative age results – vertical method.

Cluster 1	[Fe/H]	[α/Fe]	$\Delta V_{\rm TO}^{\rm HB}$	Cluster 2	[Fe/H]	[α/Fe]	$\Delta V_{\rm TO}^{\rm HB}$	τ_1/τ_2
ESO 121-SC03	-1.009	$+0.00$	3.26 ± 0.06	47 Tuc	-0.832	$+0.30$	3.56 ± 0.06	0.75 ± 0.09
ESO 121-SC03	-1.009	$+0.30$	3.26 ± 0.06	47 Tuc	-0.832	$+0.30$	3.56 ± 0.06	0.73 ± 0.09
ESO 121-SC03	-1.009	$+0.00$	3.26 ± 0.06	Pal. 12	-0.832	$+0.00$	3.32 ± 0.06	0.99 ± 0.11
ESO 121-SC03	-1.009	$+0.30$	3.26 ± 0.06	Pal. 12	-0.832	$+0.00$	3.32 ± 0.06	0.97 ± 0.11
Pal. 12	-0.832	$+0.00$	3.32 ± 0.06	47 Tuc	-0.832	$+0.30$	3.56 ± 0.06	0.76 ± 0.09

three clusters. The results may be seen in Table 6. In these calculations, we adopted [Fe/H] $\simeq -0.8$ for Pal. 12, as discussed in Section 3.2. That is, we used the [Fe/H] $= -0.83$ and [α/Fe] $= 0.0$ polynomial fit (see Table 4) for this cluster. For 47 Tuc we used the [Fe/H] $= -0.83$ and [α/Fe] $= +0.3$ polynomial fit, while for ESO 121-SC03 we adopted the polynomials with [Fe/H] $= -1.01$ and [α/Fe] $= 0.0$ or $+0.3$.

As suspected from close examination of Fig. 6, we found that varying the α-element abundance for ESO 121-SC03 does not result in large variations of the relative ages derived for this cluster via the vertical method. ESO 121-SC03 is 74 ± 9 per cent as old as 47 Tuc, and almost identical in age to Pal. 12. In order to compare our results with previous work, we also derived the age of Pal. 12 relative to 47 Tuc. We found that Pal. 12 is 76 ± 9 per cent the age of 47 Tuc, which is consistent with previous measurements. For example, Rosenberg et al. (1998) found Pal. 12 to have an age 68 ± 10 per cent that of 47 Tuc, using a horizontal indicator and several different sets of theoretical calibrations.

In order to place our relative age measurements on an absolute scale, we consider previous age determinations for 47 Tuc. One of the most recent studies, that of Gratton et al. (2003), derived an age ~ 2.6 Gyr younger than NGC 6397 and NGC 6752, which apparently represent the oldest population in the Galactic globular cluster system, with ages $13.4 \pm 0.8 \pm 0.6$ Gyr (where the first error bar accounts for random effects, and the second for systematic errors). According to this estimate, 47 Tuc has an age ~ 81 per cent that of the oldest Galactic globulars. This is reasonably consistent with the relative age studies of Rosenberg et al. (1999), who found an age ~ 90 per cent those of NGC 6937 and NGC 6752, and Salaris & Weiss (2002), who found an age ~ 87 per cent those of NGC 6937 and NGC 6752. In contrast, the recent relative age study of De Angeli et al. (2005) did not find 47 Tuc to be any younger than the oldest Galactic globulars (including NGC 6397 and NGC 6752), using both HST/WFPC2 and ground-based photometry.

If the oldest Galactic globular clusters are indeed ~ 13.4 Gyr old, and 47 Tuc is ~ 15 per cent younger than these objects, then we find ESO 121-SC03 must have an absolute age of 8.4 ± 1.0 Gyr, according to our vertical method measurements. Similarly, Pal. 12 must be 8.6 ± 1.0 Gyr old. Conversely, if 47 Tuc is just as old as the oldest Galactic globulars, then ESO 121-SC03 is 9.9 ± 1.2 Gyr old, and Pal. 12 is 10.2 ± 1.2 Gyr old. These results for ESO 121-SC03 are entirely consistent with the age estimates of Mateo et al. (1986), who found this cluster to be 10 ± 2 Gyr old if the LMC distance modulus is 18.2, or 8 ± 2 Gyr old if the LMC distance modulus is 18.7. Similarly, Bica et al. (1998) found an age of 8.5 Gyr from Washington photometry.

4.3 Results: horizontal method

On each of the three cluster CMDs we located the point on the RGB 2.2 mag brighter than our measured MSTO level, and estimated the colour by eye. Given the narrowness of the RGB sequences below the HB level, it was straightforward to obtain these measurements with an accuracy better than 0.01 mag. In fact, via some experimentation we estimate errors of ± 0.005 mag in this colour. We then calculated $\delta(V-I)_{2.2}$. These results are listed in Table 5.

Next, we applied our theoretical age calibration in order to obtain relative age estimates from the horizontal method. The results may be seen in Table 7. As previously, we used the [Fe/H] $= -0.83$ and [α/Fe] $= 0.0$ polynomial fit for Pal. 12; the [Fe/H] $= -0.83$ and [α/Fe] $= +0.3$ polynomial fit for 47 Tuc; and the polynomials with [Fe/H] $= -1.01$ and [α/Fe] $= 0.0$ or $+0.3$ for ESO 121-SC03.

From Table 7, it can be seen that the horizontal indicator is apparently more sensitive to α-element abundance than is the vertical indicator, although we note that the supposed variation with α-abundance is of the same order as the quoted errors. Overall, using the horizontal indicator we found ESO 121-SC03 to have an age 72 ± 7 per cent that of 47 Tuc, in good agreement with our result from the vertical indicator. Similarly, ESO 121-SC03 has an age 88 ± 8 per cent that of Pal. 12. For comparison, we find Pal. 12 to be 81 ± 8 per cent of the age of 47 Tuc, which is again in

Table 7. Relative age results – horizontal method.

Cluster 1	[Fe/H]	[α/Fe]	$\delta(V-I)_{2.2}$	Cluster 2	[Fe/H]	[α/Fe]	$\delta(V-I)_{2.2}$	τ_1/τ_2
ESO 121-SC03	-1.009	$+0.00$	0.336 ± 0.007	47 Tuc	-0.832	$+0.30$	0.279 ± 0.007	0.75 ± 0.07
ESO 121-SC03	-1.009	$+0.30$	0.336 ± 0.007	47 Tuc	-0.832	$+0.30$	0.279 ± 0.007	0.68 ± 0.07
ESO 121-SC03	-1.009	$+0.00$	0.336 ± 0.007	Pal. 12	-0.832	$+0.00$	0.317 ± 0.007	0.92 ± 0.08
ESO 121-SC03	-1.009	$+0.30$	0.336 ± 0.007	Pal. 12	-0.832	$+0.00$	0.317 ± 0.007	0.83 ± 0.08
Pal. 12	-0.832	$+0.00$	0.317 ± 0.007	47 Tuc	-0.832	$+0.30$	0.279 ± 0.007	0.81 ± 0.08

agreement with the relative age we derived using the vertical indicator (76 ± 9 per cent).

Based on the absolute ages for 47 Tuc discussed earlier, we find that from our horizontal method calculations, the age of ESO 121-SC03 lies in the range $8.2 - 9.6 \pm 0.9$ Gyr.

5 DISCUSSION AND CONCLUSIONS

In this paper we have presented photometric measurements from ACS/WFC imaging of ESO 121-SC03 in the F555W and F814W passbands. The resulting CMD represents the deepest and most precise published photometry for this unique LMC globular cluster. We have also presented new ACS/WFC photometry for the accreted Sagittarius dSph globular cluster Palomar 12. Using these data, we have conducted a detailed study of the age of ESO 121-SC03. Specifically, we have derived its age relative to the comparison clusters Pal. 12 and 47 Tuc using vertical and horizontal dating methods calibrated against the stellar evolution models of VandenBerg et al. (2006). These are well sampled in metallicity and allow us to account for the uncertain run of α-elements in ESO 121-SC03, as well as the fact that Pal. 12 is deficient in α-elements compared to many Galactic globulars, including 47 Tuc.

Our main result is that ESO 121-SC03 is significantly younger than 47 Tuc, but rather similar in age to Pal. 12. This conclusion is independent of assumed α-element abundance and age-dating method. Taking a straight error-weighted mean of our age measurements yields ESO 121-SC03 to be 73 ± 4 per cent the age of 47 Tuc, and 91 ± 5 per cent the age of Palomar 12. Palomar 12 is in turn 79 ± 6 per cent as old as 47 Tuc, in good agreement with previous measurements. As discussed in Section 4.2, recent results suggest the oldest Galactic globular clusters have ages of $\simeq 13.4$ Gyr. However, there is some disagreement in the literature as to whether 47 Tuc is coeval with the oldest Galactic globulars, or ~ 15 per cent younger. This uncertainty translates to an absolute age range for ESO 121-SC03, spanning $8.3 - 9.8$ Gyr. Similarly, the absolute age of Pal. 12 lies in the range $9.0 - 10.6$ Gyr. Typical errors on all these ages are ± 1.0 Gyr.

Our new, deep photometry and precise age estimate fully confirms ESO 121-SC03 as the only known LMC cluster with an age placing it squarely within the age-gap. In this respect, it is clearly a unique object which may well be able to tell us important information about the formation and evolution of the LMC. Does this cluster represent the tail-end of ancient globular cluster formation in the LMC, just as Pal. 12 and Terzan 7 do for the Sagittarius dSph galaxy? If so, then how can we reconcile this picture and the observed metallicity of ESO 121-SC03 with its remote location in the very outer LMC halo? Other ancient globular clusters at similar radii (such as NGC 1841 and Reticulum) are considerably more metal poor.

Prompted by the observation that ESO 121-SC03 is surrounded by a field population which shares the same properties as the cluster, Bica et al. (1998) speculated that ESO 121-SC03 may represent part of a recently accreted LMC building block (or dwarf galaxy). We note however, that Dirsch et al. (2000) found the age and metallicity of this cluster to be consistent with the age-metallicity relation they derived from LMC field star observations; hence they concluded the accretion of ESO 121-SC03 not a necessity. Even so, it would clearly be of interest to examine in more detail the possibility that ESO 121-SC03 is a captured object.

By analogue with known accreted clusters in the Galactic halo (such as Pal. 12), we may expect three characteristics of ESO 121-SC03 if it is indeed a captured cluster. First it may exhibit a peculiar velocity, at odds with that expected from the observed dynamics of the LMC. Second, we may hope to observe the presence of some stream or anomalous stellar population surrounding the cluster. Finally, it may be possible that ESO 121-SC03 possesses elemental abundance patterns different to those observed in other LMC globular clusters – just as Pal. 12 has been demonstrated to possess abundance ratios unlike Galactic globular clusters or field stars, but in agreement with those observed for the Sagittarius dSph (Cohen 2004).

Regarding the first characteristic, we note that Olszewski et al. (1991) measured a radial velocity of 309 $\mathrm{km\,s^{-1}}$ for ESO 121-SC03. At a position angle (measured north through east) of $\Phi = 31^\circ$ (Schommer et al. 1992) and angular separation of 9.9° from the LMC centre, this velocity fits very well with the observed carbon star kinematics and circularly-rotating disk model summarized by van der Marel et al. (2002) in their Figure 5. The observed velocity of ESO 121-SC03 also fits well with the rotational velocities exhibited by other old outer LMC globular clusters (see Schommer et al. 1992, Figure 6d). These results suggest that ESO 121-SC03 may not be an accreted cluster, unless its parent building-block shared the kinematics characteristic of the outer regions of the LMC.

Even so, regarding the second and third points above, it would clearly be of significant interest to target the area surrounding ESO 121-SC03 with deep wide-field imaging, in order to better survey the field star populations in this region. In would also be of great value to obtain high res-

olution spectral measurements with the aim of determining abundance ratios in this cluster. Together such observations may offer important clues to the origin of ESO 121-SC03 with strong implications for the formation and evolution of the LMC.

ACKNOWLEDGEMENTS

This paper is based on observations made with the NASA/ESA Hubble Space Telescope, obtained at the Space Telescope Science Institute, which is operated by the Association of Universities for Research in Astronomy, Inc., under NASA contract NAS 5-26555. These observations are associated with program #9891. ADM is grateful for financial support from a PPARC Postdoctoral Fellowship. Many thanks also to Francesca de Angeli for useful discussions about blue stragglers, and the anonymous referee whose comments helped improve the paper.

REFERENCES

Armandroff T. E., Da Costa G. S., 1991, AJ, 101, 1329
Bekki K., Couch W. J., Beasley M. A., Forbes D. A., Chiba M., Da Costa G. S., 2004, ApJ, 610, L93
Bica E., Clariá J. J., Dottori H., Santos Jr. J. F. C., Piatti A. E., 1996, ApJS, 102, 57
Bica E., Geisler D., Dottori H., Clariá J. J., Piatti A. E., Santos Jr. J. F. C., 1998, AJ, 116, 723
Binney J., Tremaine S., 1987, Galactic Dynamics. Princeton Univ. Press, Princeton, NJ
Brown J. A., Wallerstein G., Zucker D., 1997, AJ, 114, 180
Burstein D., Heiles C., 1982, AJ, 87, 1165
Carney B. W., 1996, PASP, 108, 900
Chaboyer B., 1999, in Heck A., Caputo F., eds., Post-*Hipparcos* Cosmic Candles. Kluwer, Dordrecht, p. 111
Cohen J. G., 2004, AJ, 127, 1545
Da Costa G. S., Armandroff T. E., 1990, AJ, 100, 162
Da Costa G. S., Armandroff T. E., 1995, AJ, 109, 2533
De Angeli F., Piotto G., Cassisi S., Busso G., Recio-Blanco A., Salaris M., Aparicio A., Rosenberg A., 2005, AJ, 130, 116
Dirsch B., Richtler T., Gieren W. P., Hilker M., 2000, A&A, 360, 133
Djorgovski S. G., 1993, in Djorgovski S. G., Meylan G., eds., ASP Conf. Ser. 50, Structure and Dynamics of Globular Clusters. Astron. Soc. Pac., San Francisco, p. 373
Dolphin A. E., 2000, PASP, 112, 1383
Geisler D., Bica E., Dottori H., Clariá J. J., Piatti A. E., Santos Jr. J. F. C., 1997, AJ, 114, 1920
Gratton R. G., Ortolani S., 1988, A&AS, 73, 137
Gratton R. G., Bragaglia A., Carretta E., Clementini G., Desidera S., Grundahl F., Lucatello S., 2003, A&A, 408, 529
Harris W. E., 1996, AJ, 112, 1487
Hill V., François P., Spite M., Primas F., Spite F., 2000, A&A, 364, L19
Johnson J. A., Bolte M., Hesser J. E., Ivans I. I., Stetson P. B., 2004, in McWilliam A., Rauch M., eds., Origin and Evolution of the Elements, from the Carnegie Observatories Centennial Symposia. Carnegie Observatories, Pasadena, p. 29
Johnson J. A., Bolte M., Stetson P. B., Hesser J. E., Somerville R. S., 1999, ApJ, 527, 199
Mackey A. D., Gilmore G. F., 2003a, MNRAS, 338, 85
Mackey A. D., Gilmore G. F., 2003b, MNRAS, 340, 175
Mackey A. D., Gilmore G. F., 2004, MNRAS, 352, 153
Mateo M., Hodge P., Schommer R. A., 1986, ApJ, 311, 113
Olsen K. A. G., Hodge P. W., Mateo M., Olszewski E. W., Schommer R. A., Suntzeff N. B., Walker A. R., 1998, MNRAS, 300, 665
Olszewski E. W., Schommer R. A., Suntzeff N. B., Harris H. C., 1991, AJ, 101, 515
Piotto G., De Angeli F., King I. R., Djorgovski S. G., Bono G., Cassisi S., Meylan G., Recio-Blanco A., Rich R. M., Davies M. B., 2004, ApJ, 604, L109
Puzia T. H., Perrett K. M., Bridges T. J., 2005, A&A, 434, 909
Recio-Blanco A., Piotto G., de Angeli F., Cassisi S., Riello M., Salaris M., Pietrinferni A., Zoccali M., Aparicio A., 2005, A&A, 432, 851
Rich R. M., Shara M. M., Zurek D., 2001, AJ, 122, 842
Riess A., Mack J., 2004, ACS Instrument Science Report 2004-006
Rosenberg A., Saviane I., Piotto G., Held E. V., 1998, A&A, 339, 61
Rosenberg A., Saviane I., Piotto G., Aparicio A., 1999, AJ, 118, 2306
Salaris M., Weiss A., 2002, A&A, 388, 492
Sarajedini A., 1994, AJ, 107, 618
Sarajedini A., Lee Y.-W., Lee D.-H., 1995, ApJ, 450, 712
Schlegel D. J., Finkbeiner D. P., Davis M., 1998, ApJ, 500, 525
Schommer R. A., Suntzeff N. B., Olszewski E. W., Harris H. C., 1992, AJ, 103, 447
Sirianni M., et al., 2005, PASP, 117, 1049
Stetson P. B., Hesser J. E., Smith G. H., Vandenberg D. A., Bolte M., 1989, AJ, 97, 1360
VandenBerg D. A., Bergbusch P. A., Dowler P. D., 2006, ApJS, 162, 375
van der Marel R. P., Alves D. R., Hardy E., Suntzeff N. B., 2002, AJ, 124, 2639

This paper has been typeset from a TEX/ LATEX file prepared by the author.